Analytical and computational study of magnetization switching in kinetic Ising systems with demagnetizing fields

Howard L. Richards*
Center for Materials Research and Technology, Department of Physics, and Supercomputer Computations Research Institute, Florida State University, Tallahassee, Florida 32306-3016
and Department of Solid State Physics, Risø National Laboratory, DK-4000 Roskilde, Denmark

M. A. Novotny†
Supercomputer Computations Research Institute, Florida State University, Tallahassee, Florida 32306-4052
and Department of Electrical Engineering, 2525 Pottsdamer Street, Florida A&M University–Florida State University, Tallahassee, Florida 32310-6046

Per Arne Rikvold‡
Center for Materials Research and Technology, Department of Physics, and Supercomputer Computations Research Institute, Florida State University, Tallahassee, Florida 32306-3016;
Centre for the Physics of Materials and Department of Physics, McGill University, Montréal, Québec, Canada;
and Department of Fundamental Sciences, Faculty of Integrated Human Studies, Kyoto University, Kyoto, Japan
(Received 6 December 1995)

An important aspect of real ferromagnetic particles is the demagnetizing field resulting from magnetostatic dipole-dipole interactions, which causes large particles to break up into equilibrium domains. Sufficiently small particles, however, remain single domain in equilibrium. This makes them particularly promising as materials for high-density magnetic recording media. In this paper we use analytic arguments and Monte Carlo simulations to quantitatively study the effects of the demagnetizing field on the dynamics of magnetization switching in two-dimensional, single-domain, kinetic Ising systems. For systems in the weak-field ''stochastic region,'' where magnetization switching is on average effected by the nucleation and growth of a single droplet, the simulation results can be explained by a simple model in which the free energy is a function only of magnetization. In the intermediate-field ''multidroplet region,'' a generalization of Avrami's law involving a magnetization-dependent effective magnetic field gives good agreement with the simulations. The effects of the demagnetizing field do not qualitatively change the droplet-theoretical picture of magnetization switching in highly anisotropic, single-domain ferromagnetic grains, which we recently proposed [J. Magn. Magn. Mater. **150**, 37 (1995)]. [S0163-1829(96)06530-7]

I. INTRODUCTION

The ability of single-domain ferromagnets to preserve an accurate record of past magnetic fields has several important applications. For example, fine grains in lava flows preserve a record of the direction of the geomagnetic field at the time they cooled, giving valuable insight into continental drift and the dynamics of the earth's core.[1] Of more direct technological importance is the potential application of single-domain ferromagnets to magnetic recording media,[2] such as magnetic tapes and disks. Here we present a detailed, quantitative study of some of the effects that magnetostatic interactions have on the dynamics of magnetization reversal in such particles. The treatment is based on a droplet-theoretical picture of magnetization switching in highly anisotropic, single-domain ferromagnetic grains, which we recently proposed.[3]

A. Technological and experimental background

During the magnetic recording process, different regions of the recording medium are briefly exposed to strong magnetic fields, so that each grain is magnetized in the desired direction.[2] Since each grain can in principle store one bit of data, a greater storage density could ideally be achieved by a medium containing many small grains than by one containing a few large grains. However, in order to serve as reliable storage devices, the grains must be capable of retaining their magnetizations for long periods of time in weaker, arbitrarily oriented ambient magnetic fields — i.e., they must have a high coercivity and a large remanence. Since experiments show the existence of a particle size at which the coercivity is maximum (see, e.g., Ref. 4), there is a tradeoff between high storage capacity and long-term data integrity which must give rise to an optimum choice of grain size for any given material. During both recording and storage, the relationships between the magnetic field, the size of the grain, and the lifetime of the magnetization opposed to the applied magnetic field are therefore of considerable technological interest.

Fine ferromagnetic grains have been studied experimentally for many years, but until recently such particles could be observed only in powders (see, e.g., Ref. 4). This made it difficult to differentiate the statistical properties of single-grain switching from effects resulting from distributions in particle sizes, compositions, and local environments, or from interactions between grains. Techniques such as magnetic

force microscopy (MFM) (see, e.g., Refs. 5–10) and Lorentz microscopy (see, e.g., Ref. 11) now provide means for overcoming the difficulties in resolving the magnetic properties of individual single-domain particles.

B. Theoretical treatments of magnetization reversal

The standard theory of magnetization reversal in single-domain ferromagnets is due to Néel[12] and Brown.[13] In order to avoid an energy barrier due to exchange interactions between atomic moments with unlike orientations, Néel-Brown theory assumes uniform rotation of all the atomic moments in the system. The remaining barrier is caused by magnetic anisotropy,[14] which may have contributions from both the local atomic environment and the overall shape of the sample. Anisotropy makes it energetically favorable for each atomic moment to be aligned along one or more ''easy'' axes. Buckling, fanning, and curling are, like uniform rotation, theoretical relaxation processes with few degrees of freedom and global dynamics.[2,15]

Detailed descriptions of both the static and dynamic properties of fine ferromagnetic grains have typically been formulated from micromagnetic studies,[16] in which uniform rotation, buckling, fanning, and curling emerge as particularly simple switching modes. This method involves coarse-graining the physical lattice onto a computational lattice and then solving the partial differential equations for the evolution of magnetic structures on the computational lattice. Although micromagnetics provides a good treatment for the anisotropy and demagnetizing fields, it treats thermal effects rather crudely, usually just by making the domain-wall energy temperature-dependent. A somewhat better approximation for thermal fluctuations within the underlying differential equations is to include small fluctuations using a Langevin noise term.[17] An even better treatment for thermal and time-dependent effects on the microscopic scale, is Monte Carlo simulation (see, e.g., Refs. 3, 18–24). Even when the physical phenomena can be accurately simulated, however, it will be difficult to understand the results without an adequate theoretical basis.

For materials with sufficiently high anisotropy, we recently proposed an alternative mode of relaxation with typically much shorter lifetimes than predicted for uniform rotation.[3] This picture of the switching process is based on the statistical-mechanical droplet theory for the decay of metastable phases. Small regions of the phase in which the magnetization is parallel to the applied magnetic field (the ''stable'' phase) are continually created and destroyed by thermal fluctuations within the phase in which the magnetization is antiparallel to the field (the ''metastable'' phase). As long as such a region (henceforth referred to as a ''droplet'') is sufficiently small, the short-ranged exchange interaction with the surrounding metastable phase imposes a net free-energy penalty, and the droplet will, with high probability, shrink and vanish. Should the droplet become larger than a critical size, however, this penalty will be less than the benefit obtained from orienting parallel to the magnetic field, and this ''supercritical'' droplet will with a high probability grow further, eventually consuming the grain.

In systems dominated by short-range interactions, the critical droplet radius is inversely proportional to the applied field, whereas the growth velocity of the supercritical droplets is proportional to the field, and the nucleation rate for critical droplets decreases exponentially as the inverse field increases. The nature of the metastable decay therefore depends on the relative sizes of the grain, the critical droplet, the average distance between droplets, and the lattice constant in a rather complicated fashion, as discussed in detail, e.g., in Refs. 25–28. For sufficiently small grains or weak fields, the decay occurs via a *single* droplet or system-spanning slab, which grows to fill the whole grain before another critical fluctuation has time to appear. Since the critical droplet nucleates randomly in time, this has been termed the ''stochastic'' decay region.[26] For somewhat larger grains or stronger fields, however, the nucleation rate is sufficiently high that many new droplets are likely to nucleate while the first one is still growing. This has been termed the ''multi-droplet'' decay region.[26] In Fig. 1 we sketch the regions of the space of magnetic fields and particle sizes distinguished by these different behaviors during metastable decay. Snapshots of simulations, illustrating typical corresponding spin configurations, are shown in Fig. 2. For a more complete, recent review of the droplet theory of metastable decay, see Ref. 28.

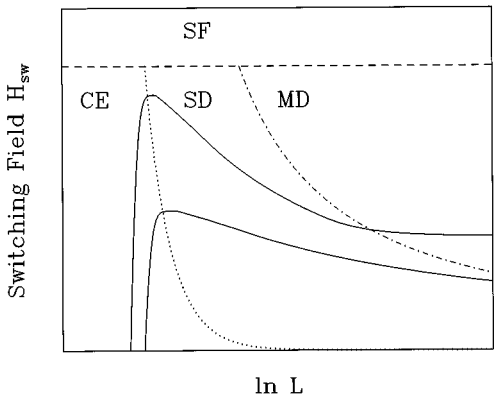

FIG. 1. The relationship between the applied field H and the system width L for a shorter (top solid curve) and a longer (bottom solid curve) fixed lifetime in a typical metastable magnetic system. Four regions are distinguished by differing decay processes: the coexistence (CE) region, the single-droplet (SD) region, the multi-droplet (MD) region, and the strong-field (SF) region. The CE and SD regions, which together form the stochastic region, are separated by the thermodynamic spinodal (dotted curve). The SD and MD regions are separated by the dynamic spinodal (dash-dotted curve). The SF region is separated from the other regions by the mean-field spinodal (dashed curve). [After Fig. 1 of Ref. 3.]

C. Kinetic Ising models and magnetostatic interactions

Because of their simplicity, kinetic nearest-neighbor Ising models have been extensively studied as prototypes for metastable dynamics (see Ref. 28 and references cited therein). Square- and cubic-lattice Ising systems with periodic boundary conditions have been used to study grain-size effects in ferroelectric switching.[29,30] Of particular significance for magnetic systems, kinetic Monte Carlo simulations of Ising and anisotropic Heisenberg systems with free boundary conditions, that give results consistent both with MFM experiments[7–10] and with the droplet-theoretical picture discussed in Sec. I B, have been performed by Serena

and Garcìa.[21] Magnetization reversal in elongated ferromagnetic particles has been studied with a one-dimensional model,[31] and a triangular-lattice Ising model with mean-field magnetostatic interactions has been shown to reproduce well the switching dynamics in Dy/Fe ultrathin films.[22]

In Ref. 3 we applied statistical-mechanical droplet theory and Monte Carlo simulations of two-dimensional Ising systems to obtain an approximation for the dynamical behavior of real single-domain particles magnetized opposite to an applied field. The results of that study were in good qualitative agreement with recent MFM experiments.[5–10] However, several simplifying approximations were made, one of which was the absence of magnetostatic interactions.

In the present article we take magnetostatics into account by including a small demagnetizing field in an Ising system otherwise identical to the one studied in Ref. 3. We calculate analytically the effects of the demagnetizing field on the magnetization switching dynamics and compare our analytic results with large-scale Monte Carlo simulations. Specifically, for systems in the stochastic region (discussed in Sec. III), the demagnetizing fields we consider must be sufficiently small that the system consists of a single domain in equilibrium, whereas in the multidroplet region (discussed in Sec. IV) it is sufficient to have the demagnetizing field much smaller than the applied field. Some preliminary results of this study were presented in Ref. 18, and additional detail can be found in Ref. 20.

The equilibrium domain structure of two-dimensional dipole systems has been extensively investigated.[32–37] The magnetostatic dipole-dipole interaction produces a demagnetizing field, which results in the stabilization of a domain structure in large ferromagnetic particles. In the context of the present study it is essential to emphasize the difference between a droplet and a domain. Although they are both spatially contiguous regions of uniform magnetization, a domain[38] is an equilibrium feature whereas *a droplet is a strictly nonequilibrium entity,* which only exists for a limited time during the switching process.

The purpose of the present paper is to study the effects of long-range dipole-dipole interactions on the *nonequilibrium* phenomenon of magnetization switching in single-domain ferromagnetic particles. Towards this end we employ a simplified model with a demagnetizing field, in which particles in equilibrium can have only one or two domains, and we emphasize the single-domain case. We obtain detailed, quantitative results and confirm that the demagnetizing field causes no qualitative modifications to the droplet-theoretical picture of magnetization switching.

The organization of the remainder of this paper is as follows. In Sec. II we define the model and present the numerical methods employed. In Sec. III we discuss the stochastic region in terms of an approximate free-energy functional and give analytical and numerical results. In Sec. IV we generalize Avrami's law,[39–41] which describes magnetization switching in the multidroplet region, to include the effects of the demagnetizing field, and we compare the analytical results to numerical simulations. Section V contains conclusions, discussions, and some directions for further work.

II. MODEL AND NUMERICAL METHODS

A. Ising model with a demagnetizing field

The standard Ising model is defined by the Hamiltonian

$$\mathcal{H}_0 = -J\sum_{\langle i,j\rangle} s_i s_j - HL^d m, \tag{1}$$

where $s_i = \pm 1$ is the z component of the magnetization of the atom (spin) at site i, $J>0$ is the ferromagnetic exchange interaction, and H is the applied magnetic field times the single-spin magnetic moment. The sum $\Sigma_{\langle i,j\rangle}$ runs over all nearest-neighbor pairs on a square (generally d-dimensional hypercubic) lattice of side L. In this work we do not consider the effects of grain boundaries, so periodic boundary conditions are imposed. (For recent Monte Carlo simulations of Ising and Heisenberg systems with open boundary conditions, see Ref. 21.) The dimensionless system magnetization is given by

$$m = L^{-d}\sum_i s_i, \tag{2}$$

where the sum is over all L^d sites. The lattice constant is set to unity.

Addition of dipole-dipole interactions gives a total Hamiltonian (SI units)

$$\mathcal{H}_{\rm dip} = \mathcal{H}_0 + \frac{\mu_0 M^2}{4\pi}\sum_{i\neq j}\frac{s_i s_j}{|\boldsymbol{r}_{ij}|^3}\left[1-3\left(\frac{\boldsymbol{r}_{ij}}{|\boldsymbol{r}_{ij}|}\cdot\hat{\boldsymbol{z}}\right)^2\right], \tag{3}$$

where M is the saturation magnetic dipole moment density and $\boldsymbol{r}_{ij}$ is the vector from site i to site j. Unfortunately, however, the last sum in Eq. (3) slows down Monte Carlo simulations significantly, which is problematic if a large number of realizations are desired for good statistics, as is the case in nonequilibrium studies. The last sum also would make a perturbative expansion in the demagnetizing field (adjustable by changing M or the sample shape) difficult. We therefore instead use the simpler Hamiltonian

$$\mathcal{H}_D = \mathcal{H}_0 + L^d D m^2. \tag{4}$$

The demagnetizing factor D, which is proportional to the demagnetizing field, is a function of the crystal symmetry, the shape of the system, and M. Equations (3) and (4) are equivalent for general ellipsoids *uniformly* magnetized along a principal axis. For the special case of a perpendicularly magnetized plane with square-lattice symmetry, $D = \frac{2}{3}\mu_0 M^2$. For nonuniformly magnetized systems, Eq. (4) amounts to a mean-field treatment of the effects of the dipole-dipole interactions. Due to the long-range nature of the dipole-dipole interactions, this is a reasonable approximation.[22,28]

For systems with periodic boundary conditions, the exchange and dipole terms of Eq. (4) are equal when the system size is given by[32]

$$L_D \approx \frac{2\sigma_\infty(T)}{D[m_{\rm sp}(T)]^2}, \tag{5}$$

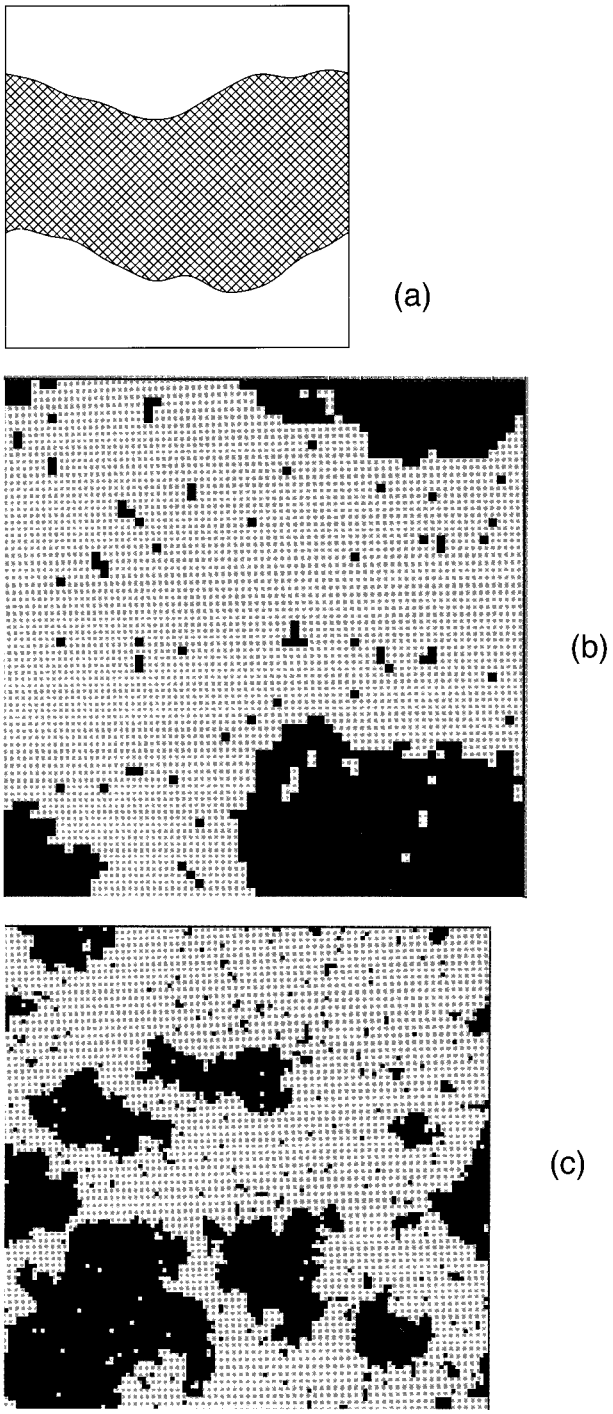

FIG. 2. Configurations that may occur during the reversal process. As in the text, periodic boundary conditions are imposed. (a) A sketch of a ''slab'' configuration. (b) A typical realization of a single droplet in the process of overtaking the system. (The droplet appears ''chopped up'' because of the periodic boundary conditions.) Grey squares are ''up'' spins and black squares are ''down'' spins. Here $L=60$, $H=-0.08J$, $D=0$, $T=0.8T_c$, and $t=410$ MCSS. [Figure courtesy of S. W. Sides.] (c) A typical realization showing the nucleation and growth of several droplets in the process of switching the magnetization. Here $L=120$, $H=-0.2J$, $D=0$, $T=0.8T_c$, and $t=114$ MCSS. [Reproduced from Fig. 5(b) of Ref. 3.]

where $\sigma_\infty(T)$ is the surface tension along a primitive lattice vector in the limit $L\to\infty$ and $m_{\rm sp}(T)$ is the spontaneous magnetization. For the two-dimensional Ising model, $\sigma_\infty(T)$ (Ref. 42) and $m_{\rm sp}(T)$ (Ref. 43) are known exactly. The length scale on which we would expect a transition from a single-domain to a multidomain equilibrium structure is approximately L_D.

The selection of the Ising model is equivalent to requiring a very large (infinite, in fact) anisotropy constant. Although magnetic materials used in magnetic recording media require comparatively large anisotropy constants,[2] the microscopic anisotropy tends to be much smaller than the exchange energy. However, in some applications, such as many thin films, it is convenient to use Ising spins to represent the individual grains which are superferromagnetically coupled to make up the system (see, e.g., Refs. 22, 44, 45). If these coupled grains reverse their magnetization through coherent rotation, as in Néel-Brown theory,[12,13] the anisotropy barrier for a *grain* is the product of the anisotropy barrier for a *single atom* and the grain volume. Thus, although this work is intended as a step towards a quantitative microscopic theory, it may equally be used to describe superferromagnetically coupled grains.

Simplicity is our main reason for choosing the two-dimensional Ising model with periodic boundary conditions, particularly since many equilibrium properties of the two-dimensional Ising model in zero field are known exactly[42,43] and since the kinetics of metastable decay has been extensively studied for this model.[28] As a result, our model systems may more closely resemble ultrathin magnetic films with perpendicular magnetization than magnetic grains. A study of three-dimensional systems is in progress,[46] but we emphasize that droplet theory should apply to almost any spin model with high anisotropy. Accordingly, equations in this paper are written in forms appropriate for arbitrary dimensionality d, even though simulations are only carried out for $d=2$.

B. Simulation of the switching dynamics

The relaxation kinetics is simulated by the single-spin-flip Metropolis dynamic with updates at randomly chosen sites. Both the Metropolis[47] and Glauber[48] algorithms are spatially local, stochastic dynamics with nonconserved order parameter (the dynamic universality class of model A in the classification scheme of Hohenberg and Halperin[49]) and are therefore expected to differ only in nonuniversal features. (A derivation from microscopic quantum Hamiltonians of the Glauber dynamic in the thermodynamic limit and under somewhat restrictive conditions has been reported.[50])

In this study we use the Metropolis dynamic, which is realized both by the original Metropolis algorithm[47] and by the n-fold way algorithm.[51] (For a discussion on the equivalence of the dynamics produced by these two algorithms, see Ref. 52.) The acceptance probability in the Metropolis algorithm for a proposed flip of the spin at site α from s_α to $-s_\alpha$ is defined as

$$W(s_\alpha\to -s_\alpha)=\min[1,\exp(-\beta\Delta E_\alpha)], \tag{6}$$

where ΔE_α is the energy change due to the flip and $\beta^{-1}\equiv k_BT$ is the temperature in units of energy. The n-fold

way algorithm is similar, but involves the tabulation of energy classes. First an energy class is chosen randomly with the appropriately weighted probability. A single site is then chosen from within that class with uniform probability and flipped with probability one. The number of Metropolis algorithm steps which would be required to achieve this change is chosen from a geometric probability distribution,[52] and the time, measured in Monte Carlo steps per spin (MCSS), is incremented accordingly. The n-fold way algorithm is more efficient than the Metropolis algorithm at low temperatures, where the Metropolis algorithm requires many attempts before a change is made.

In a single-spin-flip dynamic, the magnetization can only change by a small amount from one time step to the next. The dynamical effects of the demagnetizing field thus depend only on the *change* in the magnetic part of the Hamiltonian $\mathcal{H}_D$ [Eq. (4)] between adjacent values of the magnetization. It is therefore possible to define an *effective* magnetic field

$$H_{\rm eff}(H,D,m) \equiv \frac{\partial}{\partial m}(Hm - Dm^2) = H - 2Dm. \tag{7}$$

The effective magnetic field is thus site independent. This fact makes analytic considerations significantly easier and is our principal reason for using Eq. (4) rather than Eq. (3) as our model Hamiltonian.

We study the relaxation of the dimensionless system magnetization starting from an initial state magnetized opposite to the applied field [$m(t=0)=+1,\ H<0$]. This approach has been regularly used in simulation studies of metastable decay, ever since it was introduced by Stoll and Schneider.[53] (See Ref. 28 for references.) It corresponds closely to the procedure followed in MFM switching experiments.[5–9] All simulations presented here were performed at $T=0.8T_c$, where the spontaneous magnetization in zero field is close to unity [$m_{\rm sp}(0.8T_c)=0.9544\ldots$ (Ref. 43)], while the anisotropy in the surface tension is weak.[42] Since the applied field is negative (and generally small), the stable magnetization is approximately $m_{\rm st}\approx -m_{\rm sp}$ and the metastable magnetization is $m_{\rm ms}\approx +m_{\rm sp}$. We use as an operational definition of the lifetime τ of the metastable phase the mean first-passage time to a cutoff magnetization $m=0$:

$$\tau \equiv \langle t(m=0)\rangle. \tag{8}$$

It has been observed[27] that the qualitative results discussed below are not sensitive to the cutoff magnetization as long as it is sufficiently less than $m_{\rm sp}$. Our choice of $m=0$ as the cutoff facilitates comparison with MFM experiments, which are only capable of measuring the *sign* of the particle magnetization.

A remark on notation: in this paper a numerical subscript indicates the coefficient in a Taylor expansion in D. For example, a quantity X may be expanded as $X=X_0+X_1D+X_2D^2+\cdots$. There are three exceptions from this rule. (1) The subscripts in Eq. (26) refer to an iterative process for evaluating a continued fraction. (2) The subscripts on $\Xi_0(T)$ and $\Xi_1(T)$ [Eq. (28)] indicate an expansion in H^2 and are kept for consistency with the notation in Ref. 3. (3) Dummy variables in the Appendix [e.g., Eq. (A2)] may have numerical indices as a matter of convenience.

III. THE STOCHASTIC DECAY REGION

It has been shown[54–56] that the dynamics of metastable decay in the standard two-dimensional Ising model for sufficiently weak applied field can be semiquantitatively described by a mean-field-like dynamic in which the free energy is a function only of the system magnetization. Under these circumstances switching is abrupt, with a negligible amount of time being spent in configurations with magnetizations significantly different from $m_{\rm ms}$ or $m_{\rm st}$. Switching is then also a Poisson process, with the lifetime of a metastable phase given by the typical Van't Hoff-Arrhenius form

$$\tau \propto \exp(\beta \Delta F), \tag{9}$$

where ΔF is the free-energy barrier that must be crossed in the decay process, or by a simple generalization of Eq. (9) if more than one equivalent decay path is present [see Eq. (27)]. This phenomenon, in which the entire system behaves as though it were a single magnetic moment, is known as superparamagnetism.[14,57] As a consequence of the Poisson nature of the decay process, the standard deviation of the switching time for an individual grain is approximately equal to the mean switching time, τ. Because of the random nature of switching in this region, it has been called[26,27] the ''stochastic'' region. The stochastic region is the union of a ''coexistence'' region and a ''single-droplet'' region (discussed in Secs. III B and III D, respectively).

A. The restricted free-energy function

In the spirit of Refs. 54–56 we construct an *approximate* restricted free-energy function $F(m)$ for the entire system and use Eq. (9) to illustrate the H and D dependence of the lifetime:

$$\begin{aligned} F(m) = {} & L^d D m^2 \\ & + \min\{F_{{\rm u},+}(m), F_{{\rm u},-}(m), F_{{\rm d},+}(m), F_{{\rm d},-}(m), F_{\rm sl}(m)\} \\ & - F_{\rm sl}(m=0), \end{aligned} \tag{10}$$

where $F_{\rm sl}(m)$ is the free energy of a system composed of two ''slabs'' with magnetizations near $\pm m_{\rm sp}$ [Fig. 2(a) illustrates a ''slab'' configuration], $F_{{\rm d},\pm}(m)$ is the free energy of a system with a single droplet with magnetization near $\mp m_{\rm sp}$ in a background with magnetization near $\pm m_{\rm sp}$ [Fig. 2(b) illustrates a ''single-droplet'' configuration], and $F_{{\rm u},\pm}(m)$ is the free energy of a system in a ''uniform'' phase near $m=\pm m_{\rm sp}$. Figure 3 illustrates $\beta F(m)$ for $L \ll L_D$, $L=L_D$, and $L \gg L_D$.

We approximate the free energy of a system in a ''uniform'' phase by

$$F_{{\rm u},\pm}(m) \equiv -L^d H m + L^d \frac{1}{2}\chi^{-1}(m \mp m_{\rm sp})^2, \tag{11}$$

where χ is the equilibrium susceptibility per spin. Since an exact solution for the two-dimensional Ising model in a magnetic field has not yet been found, we use instead an estimate from a series expansion,[58] so that for $T=0.8T_c$, $\chi \approx 0.05 J^{-1}$.

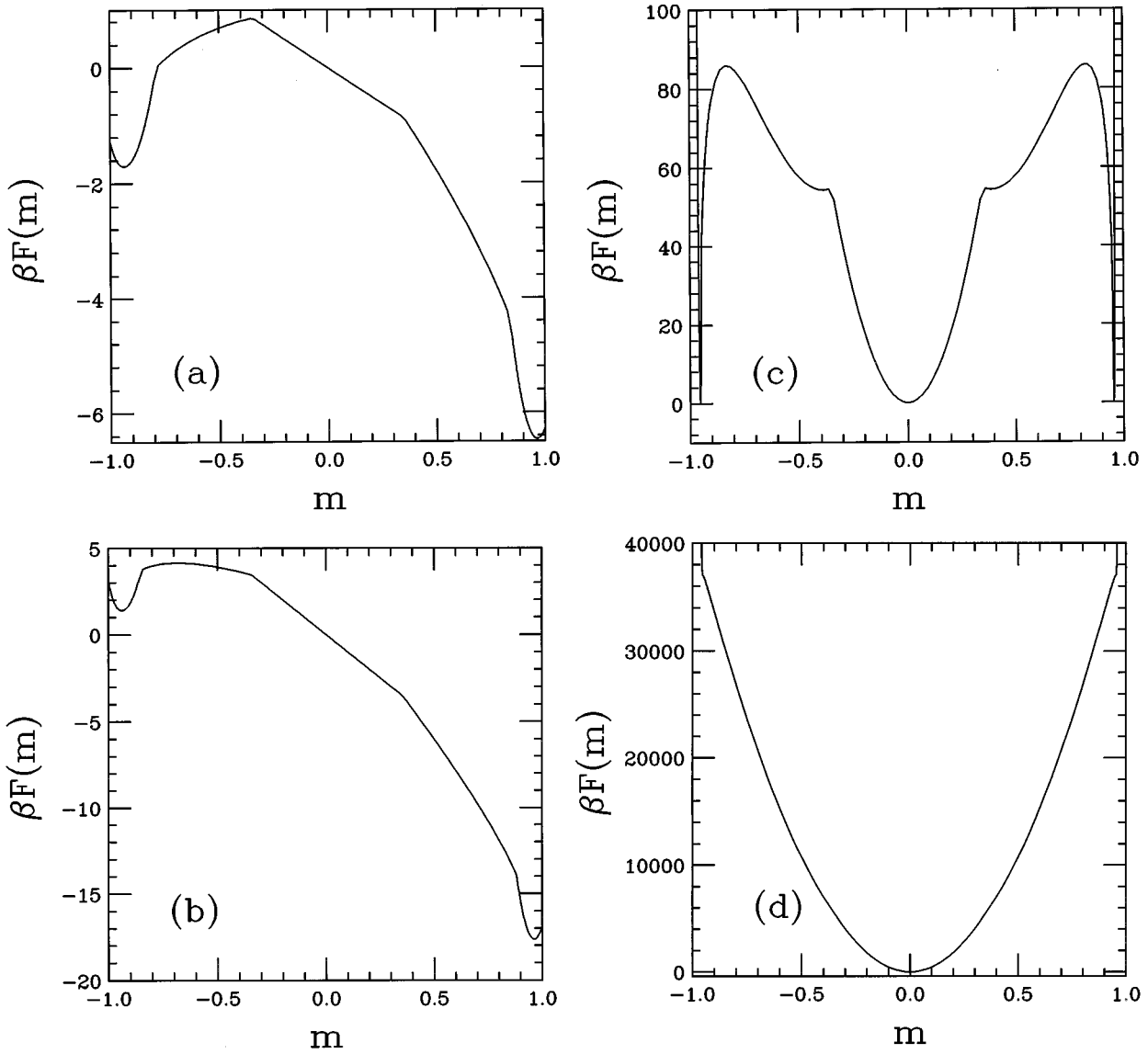

FIG. 3. The approximate restricted free energy function $F(m)$ as determined by Eq. (10) with $d=2$, $T=0.8T_c$, and $L_D=500$. (a) $L=5$, $H=0.1J$. (b) $L=10$, $H=0.1J$. (c) $L=500$, $H=0$. (d) $L=5000$, $H=0$.

Minimizing $F_{\mathrm{u},-}(m)+L^dDm^2$ yields the stable magnetization m_{st}, which is the location of the global minimum of $F(m)$ for $L<L_D$:

$$m_{\mathrm{st}}\approx\frac{-m_{\mathrm{sp}}+H\chi}{1+2D\chi} \tag{12a}$$

(remember, $H<0$). Likewise, for $L\ll L_D$ the next-lowest minimum of $F(m)$ is obtained by minimizing $F_{\mathrm{u},+}(m)+L^dDm^2$:

$$m_{\mathrm{ms}}\approx\frac{m_{\mathrm{sp}}+H\chi}{1+2D\chi}. \tag{12b}$$

Equation (12a) is valid for a wider range of H than is Eq. (12b). We shall refer to m_{ms} as the ''metastable magnetization'' and its basin of attraction as the ''metastable phase,'' since for systems of interest ($L<L_D$) the length of time required for a system initially prepared in the metastable phase to escape to the stable phase is much longer than any other time scale. Note, however, that other, shorter-lived metastable phases may exist, as discussed below.

In cases where the magnetization differs significantly from m_{sp} ($-m_{\mathrm{sp}}$), a lower free energy can often be obtained by segregating the system into a single localized ''droplet'' with magnetization near m_{st} (m_{ms}) in a background with magnetization near m_{ms} (m_{st}).[59] Specifically, the droplet free energy is approximated by

$$F_{\mathrm{d},+}(m)\equiv\Omega[d\sigma_\infty R_+^{d-1}+(m_{\mathrm{ms}}-m_{\mathrm{st}})HR_+^d]-L^dHm_{\mathrm{ms}} \tag{13a}$$

and

$$F_{\mathrm{d},-}(m)\equiv\Omega[d\sigma_\infty R_-^{d-1}-(m_{\mathrm{ms}}-m_{\mathrm{st}})HR_-^d]-L^dHm_{\mathrm{st}} \tag{13b}$$

subject to $m_{\mathrm{ms}}>m>m_{\mathrm{st}}$. Here

$$R_+ = \Omega^{-1/d} L \left(\frac{m_{\rm ms} - m}{m_{\rm ms} - m_{\rm st}} \right)^{1/d} \tag{14a}$$

is the radius of a droplet of ''down'' (stable) spins in an ''up'' (metastable) background,

$$R_- = \Omega^{-1/d} L \left(\frac{m - m_{\rm st}}{m_{\rm ms} - m_{\rm st}} \right)^{1/d} \tag{14b}$$

is the radius of a droplet of ''up'' (metastable) spins in a ''down'' (stable) background. For $T \neq 0$, the droplet shape can be found from a Wulff construction. The quantity Ω, which gives the volume of the droplet via $V = \Omega R^d$, can be found to arbitrary precision for the two-dimensional Ising model by numerically integrating over the exactly known surface tension.[60,61]

Lastly, near $m = 0$ the circumference of the droplet becomes larger than twice the cross-section of the system, and the lowest free energy is obtained by segregating the system into two slablike configurations.[62] The corresponding slab free energy is approximated by

$$F_{\rm sl}(m) \equiv 2L^{d-1}\sigma_\infty - L^d H m. \tag{15}$$

Comparison with Eq. (13) shows that $F(m) = F_{\rm sl}(m)$ for $m_{{\rm ds},+} \geqslant m \geqslant m_{{\rm ds},-}$, where[56,62]

$$m_{{\rm ds},+} = m_{\rm ms} - (m_{\rm ms} - m_{\rm st}) \Omega^{-1/(d-1)} \left(\frac{2}{d} \right)^{d/(d-1)} > 0 \tag{16a}$$

and

$$m_{{\rm ds},-} = m_{\rm st} + (m_{\rm ms} - m_{\rm st}) \Omega^{-1/(d-1)} \left(\frac{2}{d} \right)^{d/(d-1)} < 0. \tag{16b}$$

Note that for $D > H/(2m_{{\rm ds},-})$, a local minimum of $F(m)$ occurs for a slab configuration at $m = H/(2D)$. For $L < L_D$ it is a metastable phase, but for $L \geqslant L_D$ and $D > H/m_{\rm st}$ it is the global minimum of $F(m)$ and hence the true stable phase (see Fig. 3). Other interesting features can be obtained by solving $(d/dm)[L^d D m^2 + F_{{\rm d},\pm}(m)] = 0$, which can in general be done only numerically. This reveals that near $L = L_D$ short-lived metastable phases can exist for $m > m_{{\rm ds},+}$ or $m < m_{{\rm ds},-}$.

B. The coexistence region

For $L < L_D$, the system enjoys true coexistence at zero applied field between two degenerate equilibrium phases with magnetizations $m_{\rm ms}$ and $m_{\rm st}$. This leads to the identification[26,27] of a ''coexistence'' (CE) region within which $F(m_{\rm ms}) \approx F(m_{\rm st})$. Within the CE region, the free-energy barrier for tunnelling from the metastable phase to the stable phase is approximately the same as the free-energy barrier for tunnelling from the stable phase to the metastable phase, so the decay process is both stochastic and reversible. Specifically, for $L \ll L_D$, the lifetime of the metastable phase is given by Eq. (9) with $\Delta F = F(m_{{\rm ds},+}) - F(m_{\rm ms})$, so that[63–65]

$$\tau(L,H,T) \approx A(T) \exp\{\beta[2\sigma_\infty(T) L^{d-1} - L^d |H| (m_{\rm ms} - m_{{\rm ds},+}) - L^d D (m_{\rm ms}^2 - m_{{\rm ds},+}^2)]\}, \tag{17}$$

where $A(T)$ is a nonuniversal prefactor.

For $L \approx L_D$, the maximum of $F(m)$ occurs not at $m_{{\rm ds},+}$ but at a larger magnetization corresponding to a single critical droplet. The size of this droplet, however, is strongly dependent on the system size L. This part of the coexistence region is further complicated by the increasing importance of the metastable phase at $m = H/(2D)$ and the aforementioned possibility of metastable phases near $m = m_{{\rm ds},\pm}$.

C. The thermodynamic spinodal

For $|H| \gg D$ the maximum of $F(m)$ may correspond to a critical droplet the size of which is nearly independent of system size since it is determined by the *applied* field rather than the *demagnetizing* field. The applied field at which the CE region crosses over into this ''single droplet'' (SD) region has been called[26,27] the ''thermodynamic spinodal'' ($H_{\rm thsp}$). A useful estimate for this crossover is given by $(d/dm)[L^d D m^2 + F_{{\rm d},+}(m)]|_{m_{{\rm ds},+}} = 0$, which yields[56]

$$|H_{\rm thsp}| \approx L^{-1} \Omega^{1/(d-1)} \frac{(d-1)\sigma_\infty}{m_{\rm ms} - m_{\rm st}} \left(\frac{d}{2} \right)^{1/(d-1)} - 2D m_{{\rm ds},+}. \tag{18}$$

One practical indication of the thermodynamic spinodal is a peak in the switching field $H_{\rm sw}$, which is the L-dependent value of H needed to produce a fixed value of τ. (See Fig. 1.) It can be shown[20] that Eq. (17) implies that, for sufficiently large values of τ, $H_{\rm sw}(L)$ has a peak at

$$\hat{L} \equiv \left[d \frac{\ln(\tau/A)}{2\beta\sigma_\infty} \right]^{\frac{1}{d-1}}, \tag{19}$$

so that the peak occurs *precisely* on the thermodynamic spinodal as given by Eq. (18). However, because $\hat{L}$ depends so weakly on τ, it is not possible to perform simulations for which finite-size effects are not important in $H_{\rm thsp}$. These finite-size effects can be compensated in a phenomenological way through reducing L by a weakly temperature dependent length on the order of unity.[20] The estimate for the thermodynamic spinodal given by Eq. (18) is to be preferred over that used in Refs. 3 and 28 because it is more closely related to the free-energy barrier.

D. The single-droplet region

In the SD region the first critical droplet to nucleate almost always grows to fill the system before any other droplet nucleates. The average time required to nucleate the first droplet can be estimated from Eq. (9), where the free-energy barrier is determined from Eqs. (11) and (13a). Since the SD region is also a region of weak H and D, we can obtain a good approximation by neglecting terms of $O(\chi H_{\rm eff})$. Then the magnetization in the metastable background is $m_{\rm ms} = m_{\rm sp}$, and inside the droplet it is $m_{\rm st} = -m_{\rm sp}$. In terms of the droplet radius R, the difference between the free energy of a system containing one droplet and that of a uniform metastable system can then be written as

$$\Delta F(R) = d\Omega\sigma_\infty(T) R^{d-1} - 2m_{\rm sp}(|H| + 2Dm_{\rm sp}) \Omega R^d + 4D m_{\rm sp}^2 L^{-d} \Omega^2 R^{2d}. \tag{20}$$

Differentiating with respect to R, we find the implicit equation satisfied by the critical droplet radius:

$$R_c(T,H,D)=\frac{(d-1)\sigma_\infty(T)}{2m_{\rm sp}|H_{{\rm eff},c}(H,D)|}, \tag{21a}$$

where

$$|H_{{\rm eff},c}(H,D)|=|H|+2Dm_{\rm sp}[1-2\Omega(R_c/L)^d] \tag{21b}$$

is the effective field evaluated at the magnetization of a system containing a single, critical droplet. Note that $H_{{\rm eff},c}$ depends on $|H|$ and D explicitly, as well as implicitly through R_c. For $D=0$, Eq. (21) reduces to the standard expression for R_c.[28] By inserting R_c into Eq. (20) one finds that the free-energy barrier corresponding to the critical droplet is also simply given by a standard expression,[28] in which $|H|$ has been replaced by $|H_{{\rm eff},c}|$:

$$\beta\Delta F_{\rm SD}=\frac{\Xi_0(T)}{|H_{{\rm eff},c}(H,D)|}, \tag{22}$$

where[28]

$$\Xi_0(T)\equiv\beta\Omega[\sigma_\infty(T)]^d\left(\frac{d-1}{2m_{\rm sp}}\right)^{d-1}. \tag{23}$$

Note that $\Xi_0(T)$ is completely defined by quantities that for the two-dimensional Ising model are either known exactly (σ_∞ and $m_{\rm sp}$),[42,43] or can be obtained by numerical integration of exactly known quantities (Ω).[60,61]

The above results indicate that in order to obtain the nucleation rate for nonzero D, one only needs to determine $|H_{{\rm eff},c}|$. This can easily be done to arbitrary numerical precision via a rapidly convergent, generalized continued-fraction expansion as follows.

Let $x=2Dm_{\rm sp}/|H|$ be the reduced demagnetizing field and $V(x)=2\Omega(R_c/L)^d$ be the volume fraction occupied by the critical droplet. Then

$$|H_{{\rm eff},c}|=|H|\{1+x[1-V(x)]\}\equiv|H|y(x), \tag{24}$$

and $V(x)$ is given by the generalized continued-fraction expansion,

$$V(x)=\cfrac{V_0}{\left[1+x\left(1-\cfrac{V_0}{\left[1+x\left(1-\cfrac{V_0}{[\cdots]^d}\right)\right]^d}\right)\right]^d}, \tag{25}$$

where $V_0=V(0)$. This expansion can be evaluated to desired precision by the recursion relation,

$$V_n=\frac{V_0}{[1+x(1-V_{n-1})]}. \tag{26}$$

(Here the subscript is proportional to the order of a rational-fraction approximation to the generalized continued fraction, rather than denoting the order of a term in a power series in D, as elsewhere in this paper.)

The lifetime in the SD region can be given in terms of the nucleation rate per unit volume I by[28]

$$\tau\approx[L^dI]^{-1}. \tag{27}$$

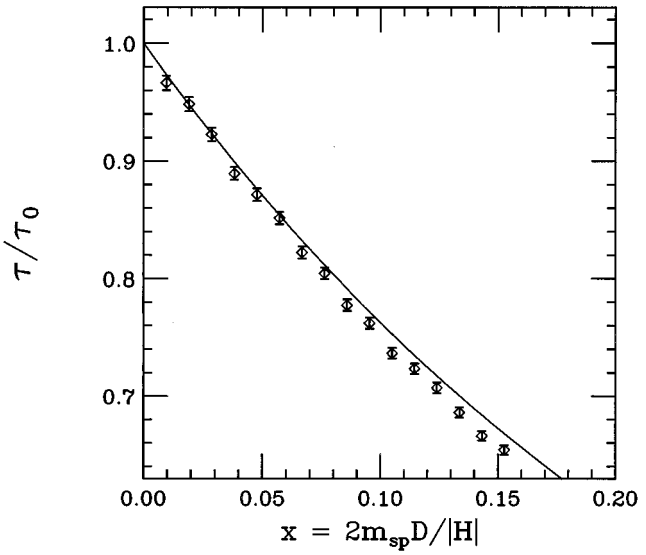

FIG. 4. The relative lifetime vs $x=2m_{\rm sp}D/|H|$ in the SD region as given by Eq. (29). $|H|=0.2J$, $T=0.8T_c$, and $L=10$. Each Monte Carlo point represents 47 500 decays. The only parameter which is not exactly known, Ξ_1, was obtained in Ref. 3 from data at $D=0$ and is *not* the result of a fit to the D-dependence.

For $D=0$ and $\chi\approx0$, I has been shown by field-theoretical arguments to be given by[28,66,67]

$$I(T,H)\approx B(T)|H|^K\exp\{-|H|^{1-d}[\Xi_0(T)+\Xi_1(T)H^2]\} \tag{28}$$

where $B(T)$ is a nonuniversal prefactor, and K should be 3 for the two-dimensional Ising model[66,67] (numerically supported by Monte Carlo[27] and transfer-matrix[68] calculations) and $-1/3$ for the three-dimensional Ising model.[67] [The subscripts on $\Xi_0(T)$ and $\Xi_1(T)$ indicate an expansion in H^2 rather than in D, and are kept for consistency with the notation in Ref. 3.] The quantity $\Xi_0(T)$ is given by Eq. (23), and we determine $\Xi_1(T)$ from a numerical fit to the H dependence of the lifetime. Note that the lifetime obtained from Eqs. (27) and (28) is quite similar to the Van't Hoff-Arrhenius form with the free-energy barrier given by Eq. (22). The only differences are the prefactor $|H|^{-K}$ and the term $\Xi_1(T)H^2$ in the exponential, which are due to surface fluctuations on the droplet and to higher-order terms in a field-theoretical calculation of the free-energy barrier, respectively.[67] We generalize to the $D\neq0$ case by assuming that the nucleation rate in the SD region is given by Eq. (28) with $|H|$ replaced by $|H_{{\rm eff},c}(H,D)|$, as we have already shown in Eq. (22) for the dominant term in the free-energy barrier, $\Delta F_{\rm SD}$. The resulting expression for the relative lifetime for nonzero D is then given by

$$\frac{\tau(x)}{\tau(0)}=y(x)^{-K}\exp\{-\Xi_0|H|^{1-d}[1-y(x)^{1-d}] -\Xi_1|H|^{3-d}[1-y(x)^{3-d}]\}, \tag{29}$$

where $y(x)$ is defined in Eq. (24). This result is shown in Fig. 4, together with Monte Carlo data, for $d=2$, $T=0.8T_c$, $|H|=0.2J$, and $L=10$. Except for Ξ_1, the parameters needed to evaluate $\tau(x)/\tau(0)$ are known exactly or

numerically exactly for the two-dimensional Ising model, $V_0=0.2399(1)$ and $\Xi_0=0.5062(1)$, or from field-theoretical calculations[66,67] of the nucleation rate, $K=3$. The value of Ξ_1 used to produce the data in Fig. 4, $\Xi_1=9.1(3)J^{-1}$, was obtained in Ref. 3 from the $|H|$ dependence of τ for $D=0$ in the SD region. Thus the good agreement seen in Fig. 4 between the simulation data and the theoretical prediction is *not* the result of a fit to the data, but is determined entirely from quantities that are either known exactly or measured with $D=0$.

IV. THE MULTIDROPLET DECAY REGION

For sufficiently strong fields or large systems, decay occurs through many weakly interacting droplets in the manner described by Kolmogorov,[39] Johnson and Mehl,[40] and Avrami.[41] Such decay is ''deterministic'' in the sense that the standard deviation of the switching time is much less than its mean (see Refs. 3, 26–28 for details).

The crossover between the SD region and the multidroplet (MD) region has been called[26,27] the ''dynamic spinodal'' (DSp). Since the standard deviation of the lifetime is equal to its mean in the stochastic region, we estimate this crossover by the field $H_{1/2}$ at which

$$\sqrt{\langle t^2(m=0)\rangle-\tau^2}=\frac{\tau}{2}. \tag{30}$$

For *asymptotically* large L, $H_{\mathrm{DSp}}\sim(1/\ln L)^{1/(d-1)}$;[3,27] however, prohibitively large system sizes may be required before this scaling form is observed.[56]

For even stronger fields, nucleation becomes much faster than growth and the droplet picture breaks down. The crossover to this ''strong-field'' (SF) region has been called[26,27] the ''mean-field spinodal'' (MFSp). A conservative estimate for this crossover field is obtained by setting $2R_c=1$:

$$|H_{\mathrm{MFSp}}|\approx\frac{(d-1)\sigma_\infty(T)}{m_{\mathrm{sp}}}. \tag{31}$$

Little is as yet known quantitatively about the dynamics of the decay near the mean-field spinodal and in the SF region. A study from a percolation-theoretical point of view is in progress.[69]

A. Time-dependent magnetization in the MD region

Avrami's law[39–41] gives the volume fraction of the metastable phase (or equivalently, the magnetization) for systems in which droplets nucleate with a constant rate (per unit volume) I_0 and grow at constant velocity v_0 without interacting except for overlaps. In this section we generalize Avrami's law to systems with nonzero D. This generalization allows for a nucleation rate and velocity that depend on the magnetization, and through it on time.

The time-dependent mean system magnetization $m(t)$ is given by

$$m(t)=(m_{\mathrm{ms}}-m_{\mathrm{st}})e^{-\Phi(t)}+m_{\mathrm{st}}. \tag{32}$$

Here

$$\Phi(t)\equiv\int_0^t I(t')V(t',t)dt' \tag{33}$$

is the mean volume fraction of droplets (uncorrected for overlap) and

$$V(t_1,t_2)\equiv\Omega\left[\int_{t_1}^{t_2}v(t)dt\right]^d \tag{34}$$

is the volume occupied by a droplet which nucleates at time t_1 and grows with a time-dependent radial velocity $v(t)$ until time t_2. Here $v(t)$ is the (nonuniversal) temperature-dependent radial growth velocity of a droplet, which under a Lifshitz-Allen-Cahn approximation[70–73] is proportional to the effective field in the limit of large droplets:

$$v(t)\approx\nu|H_{\mathrm{eff}}(H,D,m(t))|. \tag{35}$$

The time-dependent nucleation rate is given by $I(t)\equiv I[T,H_{\mathrm{eff}}(H,D,m(t))]$ from Eq. (28). Note how this differs from the D-dependent nucleation rate in the SD region, discussed in Sec. III D. In the SD region, the D dependence of the nucleation rate comes from the change in system magnetization from the nucleation of a single critical droplet. In the MD region, by contrast, we ignore the change in system magnetization due to the nucleation of a *single* droplet (since $L\gg R_c$), and the D dependence of the nucleation rate comes from the change in system magnetization due to an *ensemble* of supercritical droplets.

For $D=0$, Eq. (32) becomes[39–41]

$$m_0(t)=(m_{\mathrm{ms},0}-m_{\mathrm{st},0})e^{-\Phi_0(t)}+m_{\mathrm{st},0}, \tag{36}$$

where

$$\Phi_0(t)=\ln\left(\frac{m_{\mathrm{ms},0}-m_{\mathrm{st},0}}{|m_{\mathrm{st},0}|}\right)\left(\frac{t}{\tau_0}\right)^{d+1}, \tag{37}$$

so that τ_0 is the first-passage time to $m=0$ [Eq. (8)]. Specifically, τ_0 is given by[39–41]

$$\tau_0=\left[\frac{I_0\Omega v_0^d}{(d+1)\ln z_0}\right]^{(-1/d+1)}, \tag{38}$$

where

$$z_0\equiv\frac{m_{\mathrm{ms},0}-m_{\mathrm{st},0}}{|m_{\mathrm{st},0}|}\approx 2. \tag{39}$$

In Eq. (39) and elsewhere in this section, the estimate for the metastable magnetization given by Eq. (12b) does not suffice. Ramos *et al.* have estimated $m_{\mathrm{ms}}(|H|)$ by extrapolating $m(t)$ back to $t=0$ assuming that $m(t)$ is correctly described by Avrami's law.[69] (Since the initial condition is $m_0=1$ rather than $m_0=m_{\mathrm{ms}}$, the earliest times must be discarded.) These estimates are shown in Fig. 5. We fit a smooth curve through the data, insisting that $m_{\mathrm{ms}}(0)\equiv m_{\mathrm{sp}}$ and $(d/dH)m_{\mathrm{ms}}|_{H=0}=\chi$. The smooth curve allows us to estimate the change in m_{ms} due to D, but an analytic expression for $m_{\mathrm{ms}}(|H|)$ is not known.

For $D=0$, the standard deviation of the time-dependent magnetization has been shown to vanish with increasing system size as $L^{-d/2}$;[3,74] i.e., the magnetization is strongly self-averaging[75] in the MD region. This feature is shared by the more general case of $D\geqslant 0$. In fact, realizations in which the magnetization chances to decay more rapidly than average will experience a weaker effective field [Eq. (7)], and

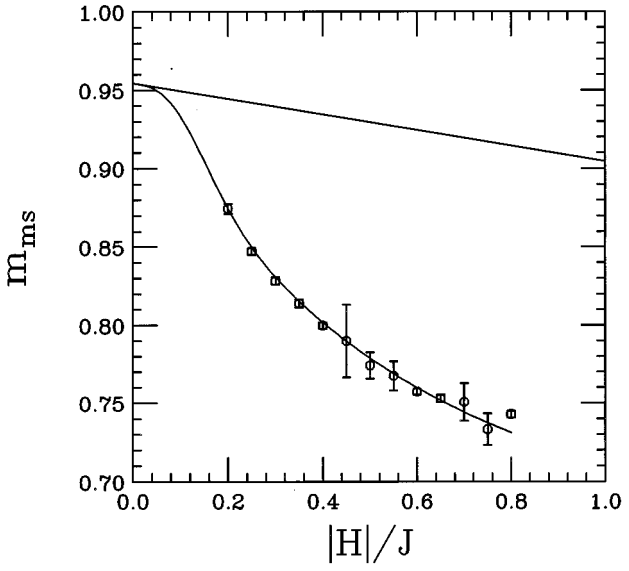

FIG. 5. The metastable magnetization vs $|H|$ in the MD region. The data points were estimated by Ramos *et al.*[69] by extrapolating the time-dependent magnetization values back to $t=0$, assuming Avrami's law. The smooth curve is a useful estimate, but an explicit expression for $m_{\rm ms}(|H|)$ is not known except near $H=0$, where Eq. (12b) applies. The straight line indicates the approximation Eq. (12b).

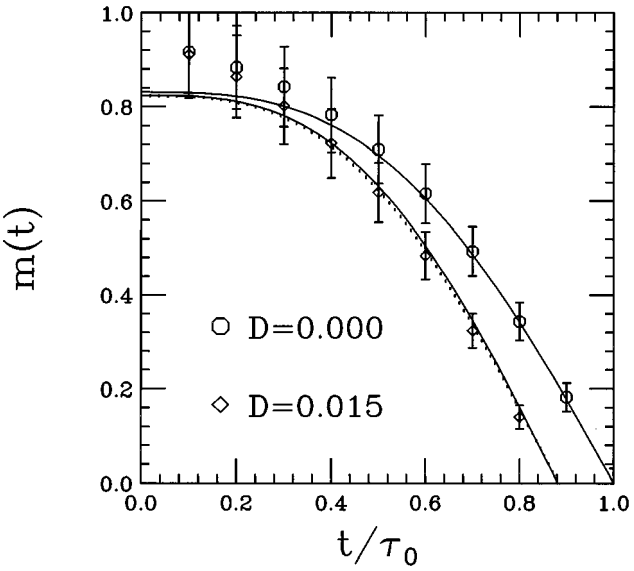

FIG. 6. The magnetization vs time in the MD region as given by Eqs. (36) and (45). $|H|=0.3J$, $T=0.8T_c$, and $L=50$. The two values of D displayed are $D=0$ and $D=0.015$. The solid curves are $m_0(t)+Dm_1(t)$; the dotted curve (hardly distinguishable on the scale of this figure) is $m_f(t)$. Each Monte Carlo point represents 100 decays.

realizations in which the magnetization decays more slowly than average will experience a stronger effective field. These effects combine to cause systems with $D>0$ to have even smaller standard deviations in their time-dependent magnetizations than corresponding systems with $D=0$.

To first order in D, the effective magnetic field [from Eq. (7)] is given by

$$H_{\rm eff}(H,D,m(t))\approx H-2Dm_0(t) \tag{40}$$

since any D-dependent terms in $m(t)$ will lead to only higher-order corrections. We will expand $\Phi(t)$ to first order in D, so that we can use the known value of $m_0(t)$ instead of the unknown value $m(t)$ on the right-hand side of Eq. (33). In order to perform the expansion correctly, we must expand $I(t)$ and $V(t_1,t_2)$ to first order in D. Specifically, the total volume fraction (uncorrected for overlap) of droplets after a time t is given by

$$\Phi(t)\approx\Phi_0(t)+\Phi_1(t)D \tag{41}$$

where

$$\Phi_1(t)\equiv\Phi_V(t)+\Phi_I(t), \tag{42}$$

with

$$\Phi_V(t)\equiv\int_0^t I_0V_1(t',t)dt' \tag{43}$$

and

$$\Phi_I(t)\equiv\int_0^t I_1(t')V_0(t',t)dt'. \tag{44}$$

Straightforward but cumbersome mathematics gives explicit expressions for $\Phi_I(t)$ and $\Phi_V(t)$ [Eqs. (A12) and (A14) in the Appendix]. These expressions are inserted into Eq. (42) to find $\Phi_1(t)$, and Eq. (32) is used to evaluate

$$m_1(t)=(m_{\rm ms,1}-m_{\rm st,1})e^{-\Phi_0(t)}+m_{\rm st,1}-(m_{\rm ms,0}-m_{\rm st,0})e^{-\Phi_0(t)}\Phi_1(t). \tag{45}$$

Finding the second-order terms in D proceeds along parallel lines. Although it is possible to find an analytic expression for $m_2(t)$, this expression is tedious to derive and unenlightening. Furthermore, enough approximations have already been introduced to make the significance of an analytic expression for $m_2(t)$ suspect. Consequently, we estimate $m(t)$ by integrating Eq. (33) numerically with the effective field $H-2D[m_0(t)+Dm_1(t)]$. The resulting estimate we denote $m_f(t)$, and it should be approximately correct to $O(D^2)$. If necessary, this process can be iterated to find successively better approximations for $m(t)$.

Figure 6 shows the time-dependence of the the magnetization, both as approximated above and as simulated by Monte Carlo. For Ξ_1 we have used $\Xi_1=3.0(3)$, as determined in Ref. 3 from the $|H|$ dependence of τ for $D=0$ in the MD region. Note that there is good agreement between the simulation results and the approximation after an initial relaxation into the metastable phase, and that the modification to $m(t)$ resulting from higher-order terms is minor.

B. Lifetime in the MD region

In order to calculate the effect of D on the lifetime, we start with $m(\tau)\equiv 0$ and expand both m and τ in D. Collecting terms and discarding all terms of higher order than D^2, we find

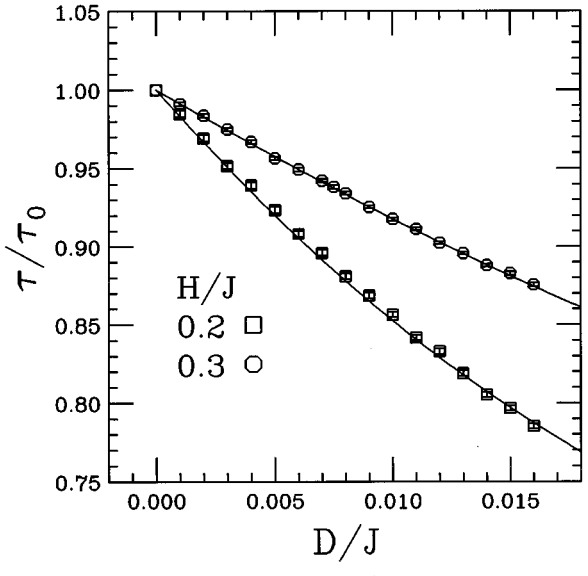

FIG. 7. The lifetime vs D in the MD region for $T=0.8T_c$ with $|H|=0.2J$ and $|H|=0.3J$. The solid curves represent the theoretical predictions given by combining Eqs. (47) and (48) and are *not* the result of a fit to the D dependence. Each Monte Carlo point represents at least 5 000 decays in a system of size $L=100$. [Reproduced from Fig. 4 of Ref. 18.]

$$0=\{m_0(\tau_0)\}+\left\{m_1(\tau_0)+\tau_1\frac{dm_0}{dt}\bigg|_{\tau_0}\right\}D+\left\{m_2(\tau_0)+\tau_1\frac{dm_1}{dt}\bigg|_{\tau_0}+\tau_2\frac{dm_0}{dt}\bigg|_{\tau_0}+\frac{1}{2}\tau_1^2\frac{d^2m_0}{dt^2}\bigg|_{\tau_0}\right\}D^2. \tag{46}$$

Since the quantities in the braces are independent of D and Eq. (46) is true for all small D, by necessity $m_0(\tau_0)=0$,

$$\tau_1=-m_1(\tau_0)\left[\frac{dm_0}{dt}\bigg|_{\tau_0}\right]^{-1}, \tag{47}$$

and

$$\tau_2=-\left[m_2(\tau_0)+\tau_1\frac{dm_1}{dt}\bigg|_{\tau_0}+\frac{1}{2}\tau_1^2\frac{d^2m_0}{dt^2}\bigg|_{\tau_0}\right]\left[\frac{dm_0}{dt}\bigg|_{\tau_0}\right]^{-1}. \tag{48}$$

Equation (47) is readily evaluated because $\Phi_0(t)$ is a simple function. It is likewise simple to calculate $(d^2m_0/dt^2)|_{\tau_0}$ for use in Eq. (48). We have not actually solved for $m_2(t)$, but for small D we can use

$$m_2(t)\approx D^{-2}\{m_f(t)-[m_0(t)+Dm_1(t)]\}. \tag{49}$$

Finally, $(dm_1/dt)|_{\tau_0}$ can be evaluated by differentiating $\Phi_V(t)$ [Eq. (A12)] and $\Phi_I(t)$ [Eq. (A14)] with respect to t. The results are given in Eqs. (A15) and (A16) in the Appendix, respectively. Inserting these in Eq. (42) we obtain $(d\Phi_1/dt)|_{\tau_0}$. Once this is known, differentiating Eq. (45) is trivial, and τ_2 can easily be evaluated.

Figure 7 shows τ vs D for two different values of H. The agreement between the theoretical curves and the Monte Carlo data is again excellent. Once again, the theoretical curves are not fits to the simulation data, but in addition to exactly known quantities use only parameters determined for $D=0$, namely, $m_{\rm ms}(|H|)$ (Ref. 69) and $\Xi_1(T)$.[3]

V. DISCUSSION

Due to the importance of magnetic recording technologies in modern society, magnetic relaxation has been a subject of study for many years. However, even the equilibrium thermodynamics of magnetic materials is very difficult to predict from first principles and generally has to be approximated from simpler models (see, e.g., Ref. 76). As a result, the most popular method for theoretical investigation of magnetization reversal involves setting up and solving differential equations on a lattice obtained by coarse graining over the microscopic crystal lattice. This method, known as micromagnetics,[16] often gives very good results, particularly for equilibrium studies or for multidomain particles. However, micromagnetic calculations take thermal effects into account only crudely.

An alternative method is to treat the statistical mechanics carefully, making simplifications to the model until it can be well understood. This is the approach we take. In Ref. 3 we showed that both the switching field and the probability that the magnetization has not changed sign within a given time, calculated from Monte Carlo simulations of the two-dimensional Ising model, are qualitatively similar to the same quantities measured in isolated, well characterized single-domain ferromagnets by techniques such as MFM. Since statistical-mechanical droplet theory successfully explains the Ising model simulations, it is plausible that droplet theory could also be applied to the experiments.

In this article we consider the effect of the magnetic dipole-dipole interaction, which was neglected in Ref. 3. By treating the dipole-dipole interaction in a mean-field approximation, we are able to calculate droplet-theory predictions for the lifetime for systems in which magnetic decay occurs by means of a single droplet (Fig. 4). We also obtain both the time-dependent magnetization (Fig. 6) and the lifetime (Fig. 7) for systems in which magnetic decay occurs through the action of many droplets. In all of these calculations, all parameters were either known exactly or determined by measurements at $D=0$, so the excellent agreements between our analytical expressions and the simulation data are not the results of curve fitting.

It should be pointed out that the droplet-theory predictions made in both the single-droplet and multidroplet regions are large-droplet approximations. Since a critical droplet in the two-dimensional Ising model at $T=0.8T_c$ and $|H|=0.3J$ consists of approximately six overturned spins, it is quite remarkable that these expressions give the good approximations they do.

In Ref. 22, Kirby *et al.* use the two-dimensional Ising model with mean-field dipole-dipole interactions to simulate Dy/Fe ultrathin films which they have observed experimentally, obtaining good agreement. The analytic results from Sec. IV are directly applicable to such films, although different values of T, H, and D must be chosen to make the comparison. However, care should be used in applying the results. Specifically, if $|Dm_{\rm sp}/H|$ is not small, more numerical iterations of the type described in Sec. IV will be neces-

sary, and if $|H_{\rm eff}| \gtrsim |H_{\rm MFSp}|$ [Eq. (31)], droplet theory may not be applicable.

It is a noteworthy conclusion of this study that the mean-field demagnetizing field does not change the qualitative predictions of the droplet-theoretical switching model introduced in Ref. 3. In particular, the switching field as a function of system size is qualitatively similar to that which was obtained in Ref. 3 and is sketched in Fig. 1. Although the values of the switching field are reduced, a peak in the switching field still occurs near the thermodynamic spinodal, as can be seen by comparing Eqs. (17) and (27). Furthermore, the switching field remains roughly independent of L in the MD region. What is noticeably absent is any feature at $L=L_D$: the switching field shows features due to transitions in the dynamics, but not transitions in the statics. This is because our droplet-theoretical model assumes that the system starts from a single-domain initial condition. Experimentally, the initial condition is typically prepared by applying a strong field in the $+z$ direction, but for $L \gg L_D$ this will not be sufficient to produce a single-domain state in equilibrium. Such a multidomain initial condition means that the lifetime is limited only by the growth velocity, and no longer by the nucleation rate. This greatly reduces $H_{\rm sw}$ for systems with $L \gg L_D$. However, if the ''optimum'' grain size $\hat{L}$ [given by Eq. (19)] is much smaller than L_D, there will still be a peak in $H_{\rm sw}$ due to the crossover between the CE and SD regions.

Even with the addition of the demagnetizing field, the Ising model remains too crude a model for magnetism to describe quantitatively real magnetic materials, except perhaps for some ultrathin films as noted above. Heterogenous nucleation at boundaries,[20,77] quenched disorder,[78] and more realistic anisotropies,[78] as well as extensions to three-dimensional grains[46] will therefore be subjects of future studies.

ACKNOWLEDGMENTS

The authors wish to thank B. M. Gorman and R. A. Ramos for useful discussions and for comments on the manuscript. We also wish to thank S. W. Sides for Fig. 2(b), and R. A. Ramos for providing the data on which Fig. 5 is based prior to publication. During the final stages of this work, H. L.R. and P.A.R. enjoyed the hospitality and support of the Risø National Laboratory and McGill University, respectively. P.A.R. also enjoyed the hospitality of Kyoto University, where his visit was supported by the Japan Foundation's Center for Global Partnership through National Science Foundation Grant No. INT-9512679. This research was supported in part by the Florida State University Center for Materials Research and Technology, by the FSU Supercomputer Computations Research Institute, which is partially funded by the U.S. Department of Energy through Contract No. DE-FC05-85ER25000, and by the National Science Foundation through Grants No. DMR-9315969 and DMR-9520325. Computing resources at the National Energy Research Supercomputer Center were made available by the U.S. Department of Energy.

APPENDIX: AVRAMI'S LAW FOR $D \geq 0$

In this appendix we give some of the steps that have been omitted for clarity in Sec. IV. Beginning with the Lifshitz-Allen-Cahn approximation[70–73] for the radial growth velocity [Eq. (35)] and with the effective magnetic field to $O(D)$ [Eq. (7)], we find

$$v(t) \approx v_0 \left[1 + \frac{2D}{|H|} m_0(t) \right]. \tag{A1}$$

Substituting Eq. (50) into Eq. (34), we find

$$V(t_1,t_2) \approx \Omega v_0^d \left\{ \int_{t_1}^{t_2} \left[1 + \frac{2D}{|H|} m_0(t) \right] dt \right\}^d \approx \Omega v_0^d \left[(t_2-t_1)^d + \binom{d}{1} \frac{2D}{|H|} (t_2-t_1)^{d-1} \int_{t_1}^{t_2} m_0(t)\,dt \right]. \tag{A2}$$

This enables us to make the identifications

$$V_0(t_1,t_2) = \Omega v_0^d (t_2-t_1)^d \tag{A3}$$

and

$$V_1(t_1,t_2) = 2\Omega v_0^d \binom{d}{1} |H|^{-1} (t_2-t_1)^{d-1} \int_{t_1}^{t_2} m_0(t)\,dt. \tag{A4}$$

A Taylor expansion of the nucleation rate [Eq. (28)]

$$I(t) \approx I_0 + \left. \frac{dI}{dD} \right|_0 D = I_0 + \left. \frac{dI}{d|H_{\rm eff}|} \right|_0 \left. \frac{d|H_{\rm eff}|}{dD} \right|_0 D = I_0 + \left. \frac{dI}{d|H_{\rm eff}|} \right|_0 [2m_0(t)] D \tag{A5}$$

yields

$$I_1(t) = \lambda(H) I_0 m_0(t), \tag{A6}$$

where

$$\lambda(H) \equiv 2 \left\{ \frac{K}{|H|} + |H|^{-d} [(d-1)\Xi_0 + (d-3)\Xi_1 H^2] \right\} \tag{A7}$$

comes from differentiating Eq. (28) with respect to H.

The evaluation of $\Phi_I(t)$ and $\Phi_V(t)$ can be followed more easily if the reader keeps in mind three basic ''tricks'': (i) we apply of the binomial theorem,

$$(t-t')^n = \sum_{k=0}^{n} t^k (-t')^{n-k} \binom{n}{k}, \tag{A8}$$

(ii) we use Eq. (38) to simplify expressions, and (iii) we make changes of variables of the form $x=\Phi_0(t')$. These lead to expressions such as

$$(d+1)\left(\frac{\ln z_0}{\tau_0^{d+1}}\right)^{(n+1)/(d+1)} t^k (t')^{n-k} dt' = [\Phi_0(t)]^{k/(d+1)} x^{(n-k-d)/(d+1)} dx. \tag{A9}$$

Using Eq. (36) in Eq. (53)

$$\begin{aligned} V_1(t_1,t_2) &\approx 2\Omega v_0^d \binom{d}{1} |H|^{-1} (t_2-t_1)^{d-1} |m_{\mathrm{st},0}| \int_{t_1}^{t_2} \left\{ z_0 \exp\left[-\ln(z_0) \left(\frac{t}{\tau_0} \right)^{d+1} \right] - 1 \right\} dt \\ &= 2\binom{d}{1} |H|^{-1} |m_{\mathrm{st},0}| \left[-V_0(t_1,t_2) + \Omega v_0^d \frac{z_0}{d+1} (\ln z_0)^{-1/(d+1)} (t_2-t_1)^{d-1} \tau_0 \int_{\Phi_0(t_1)}^{\Phi_0(t_2)} e^{-x} x^{1/(d+1)-1} dx \right] \\ &= 2\binom{d}{1} |H|^{-1} |m_{\mathrm{st},0}| \left(-V_0(t_1,t_2) + \Omega v_0^d \frac{z_0}{d+1} (\ln z_0)^{-1/(d+1)} (t_2-t_1)^{d-1} \right. \\ &\quad \left. \times \tau_0 \left\{ \gamma\left[\frac{1}{d+1}, \Phi_0(t_2) \right] - \gamma\left[\frac{1}{d+1}, \Phi_0(t_1) \right] \right\} \right), \end{aligned} \tag{A10}$$

where γ denotes the incomplete gamma function

$$\gamma(a,x) \equiv \int_0^x y^{a-1} e^{-y} dy. \tag{A11}$$

Using Eq. (A10) in Eq. (43),

$$\begin{aligned} \Phi_V(t) &\approx 2\binom{d}{1} |H|^{-1} |m_{\mathrm{st},0}| \left(-\Phi_0(t) + I_0 \Omega v_0^d \frac{z_0}{d+1} (\ln z_0)^{-1/(d+1)} \tau_0 \left\{ \frac{t^d}{d} \gamma\left[\frac{1}{d+1}, \Phi_0(t) \right] \right. \right. \\ &\quad \left. \left. - \int_0^t (t-t')^{d-1} \gamma\left[\frac{1}{d+1}, \Phi_0(t') \right] dt' \right\} \right) \\ &= 2\binom{d}{1} |H|^{-1} |m_{\mathrm{st},0}| \left(-\Phi_0(t) + z_0 (\ln z_0)^{d/(d+1)} \tau_0^{-d} \left\{ \frac{t^d}{d} \gamma\left[\frac{1}{d+1}, \Phi_0(t) \right] \right. \right. \\ &\quad \left. \left. - \int_0^t \sum_{k=0}^{d-1} \binom{d-1}{k} t^k (-t')^{d-1-k} \gamma\left[\frac{1}{d+1}, \Phi_0(t') \right] dt' \right\} \right) \\ &= 2\binom{d}{1} |H|^{-1} |m_{\mathrm{st},0}| \left\{ -\Phi_0(t) + \frac{z_0}{d} [\Phi_0(t)]^{d/(d+1)} \gamma\left[\frac{1}{d+1}, \Phi_0(t) \right] \right. \\ &\quad \left. + \frac{z_0}{d+1} \sum_{k=0}^{d-1} \binom{d-1}{k} (-1)^{d-k} [\Phi_0(t)]^{k/(d+1)} \mathcal{A}\left(\frac{-(k+1)}{d+1}, \frac{1}{d+1}, \Phi_0(t) \right) \right\}, \end{aligned} \tag{A12}$$

where $\mathcal{A}$ is given by

$$\mathcal{A}(a,b,x) \equiv \int_0^x y^a \gamma(b,y) dy. \tag{A13}$$

Both $\mathcal{A}$ and the incomplete gamma function γ are easily evaluated by Taylor series.

It is somewhat easier to evaluate $\Phi_I(t)$. From Eq. (44) and Eq. (A6),

$$\begin{aligned} \Phi_I(t) &= \lambda(H) I_0 \Omega v_0^d \int_0^t m_0(t') (t-t')^d dt' \\ &\approx \lambda(H) \frac{(d+1)\ln(z_0)}{\tau_0^{d+1}} |m_{\mathrm{st},0}| \left\{ -\int_0^t (t-t')^d dt' + z_0 \int_0^t \exp\left[-\ln(z_0) \left(\frac{t'}{\tau_0} \right)^{d+1} \right] (t-t')^d dt' \right\} \\ &= \lambda(H) |m_{\mathrm{st},0}| \left\{ -\Phi_0(t) + \frac{z_0(d+1)\ln(z_0)}{\tau_0^{d+1}} \int_0^t \sum_{k=0}^{d} \binom{d}{k} t^k (-t')^{d-k} \exp\left[-\ln(z_0) \left(\frac{t'}{\tau_0} \right)^{d+1} \right] dt' \right\} \\ &= \lambda(H) |m_{\mathrm{st},0}| \left[z_0 \left\{ \sum_{k=0}^{d} \binom{d}{k} (-1)^{d-k} [\Phi_0(t)]^{k/(d+1)} \int_0^{\Phi_0(t)} x^{-k/(d+1)} e^{-x} dx \right\} - \Phi_0(t) \right] \\ &= \lambda(H) |m_{\mathrm{st},0}| \left[z_0 \left\{ \sum_{k=0}^{d} \binom{d}{k} (-1)^{d-k} [\Phi_0(t)]^{k/(d+1)} \gamma\left(1 - \frac{k}{d+1}, \Phi_0(t) \right) \right\} - \Phi_0(t) \right]. \end{aligned} \tag{A14}$$

The derivatives of $\Phi_v(t)$ and $\Phi_l(t)$ with respect to t are needed to obtain τ_2 in Sec. IV B. These are obtained directly from Eqs. (A12) and (A14) above

$$\frac{d}{dt}\Phi_V(t)\big|_{t=\tau_0} \approx 2(d)|H|^{-1}|m_{\mathrm{st},0}|\,\frac{(d+1)\ln z_0}{\tau_0}\left\{-1+\frac{1}{d}\,\frac{z_0}{d+1}(\ln z_0)^{-1/(d+1)}\gamma\left(\frac{1}{d+1},\ln z_0\right)\right.$$
$$\left.+\frac{z_0}{(d+1)^2}\sum_{k=0}^{d-1}\binom{d-1}{k}(-1)^{d-k}k(\ln z_0)^{(k-d-1)/(d+1)}\mathcal{A}\left(\frac{-(k+1)}{d+1},\frac{1}{d+1},\ln z_0\right)\right\} \tag{A15}$$

and

$$\frac{d}{dt}\Phi_I(t)\big|_{t=\tau_0} \approx \lambda(H)|m_{\mathrm{st},0}|\,\frac{(d+1)\ln z_0}{\tau_0}\left[-1+\frac{z_0}{d+1}\sum_{k=0}^{d}\left\{\binom{d}{k}(-1)^{d-k}k(\ln z_0)^{(k-d-1)/(d+1)}\gamma\left(1-\frac{k}{d+1},\ln z_0\right)\right\}\right]. \tag{A16}$$

*Current address: Department of Physics, University of Tokyo, Hongo 7-3-1, Bunkyo-ku, Tokyo 113, Japan. Electronic address: richards@shpd.phys.s.u-tokyo.ac.jp

†Electronic address: novotny@scri.fsu.edu

‡Permanent address: Florida State University. Electronic address: rikvold@scri.fsu.edu

[1] D. H. Tarling, *Palaeomagnetism: Principles and Applications in Geology, Geophysics and Archaeology* (Chapman and Hall, New York, 1983).

[2] E. Köster and T. C. Arnoldussen, in *Magnetic Recording*, edited by C. D. Mee and E. D. Daniel (McGraw-Hill, New York, 1987), Vol. 1, p. 98.

[3] H. L. Richards, S. W. Sides, M. A. Novotny, and P. A. Rikvold, J. Magn. Magn. Mater. **150**, 37 (1995).

[4] E. F. Kneller and F. E. Luborsky, J. Appl. Phys. **34**, 656 (1963).

[5] Y. Martin and H. K. Wickramasinghe, Appl. Phys. Lett. **50**, 1455 (1987).

[6] T. Chang, J.-G. Zhu, and J. H. Judy, J. Appl. Phys. **73**, 6716 (1993).

[7] M. Lederman, G. A. Gibson, and S. Schultz, J. Appl. Phys. **73**, 6961 (1993).

[8] M. Lederman, D. R. Fredkin, R. O'Barr, and S. Schultz, J. Appl. Phys. **75**, 6217 (1994).

[9] M. Lederman, S. Schultz, and M. Ozaki, Phys. Rev. Lett. **73**, 1986 (1994).

[10] R. M. H. New, R. F. W. Pease, and R. L. White, J. Vac. Sci. Technol. B **13**, 1089 (1995); R. M. H. New, Ph.D. dissertation, Stanford University, 1995.

[11] C. Salling, S. Schultz, I. McFadyen, and M. Ozaki, IEEE Trans. Magn. **27**, 5184 (1991).

[12] L. Néel, Ann. Geophys. **5**, 99 (1949).

[13] W. F. Brown, J. Appl. Phys. **30**, 130S (1959); Phys. Rev. **130**, 1677 (1963).

[14] I. S. Jacobs and C. P. Bean, in *Magnetism*, edited by G. T. Rado and H. Suhl (Academic, New York, 1963), Vol. 3, p. 271.

[15] E. Kneller, in *Magnetism and Metallurgy*, edited by A. E. Berkowitz and E. Kneller (Academic, New York, 1969), Vol. 1.

[16] W. F. Brown, *Micromagnetics* (Wiley, New York, 1963); S. Shtrikman and D. Treves, in *Magnetism*, edited by G. T. Rado and H. Suhl (Academic, New York, 1963), Vol. 3, p. 395.

[17] A. Lyberatos, D. V. Berkov, and R. W. Chantrell, J. Phys. Condens. Matter **5**, 8911 (1993).

[18] H. L. Richards, S. W. Sides, M. A. Novotny, and P. A. Rikvold, J. Appl. Phys. **79**, 5749 (1996).

[19] H. L. Richards, S. W. Sides, M. A. Novotny, and P. A. Rikvold, in *Physical Phenomena at High Magnetic Fields II*, edited by R. Schrieffer, L. Gor'kov, Z. Fisk, and D. Meltzer (World Scientific, Singapore, 1996).

[20] H. L. Richards, Ph.D. dissertation, Florida State University, 1996.

[21] P. A. Serena and N. García, in *Quantum Tunneling of Magnetization – QTM'94*, edited by L. Gunther and B. Barbara (Kluwer, Dortrecht, 1995), p. 107.

[22] R. D. Kirby, J. X. Shen, R. J. Hardy, and D. J. Sellmyer, Phys. Rev. B **49**, 10 810 (1994).

[23] A. Hucht, A. Moschel, and K. D. Usadel, J. Magn. Magn. Mater. **148**, 32 (1995).

[24] S. T. Chui and D.-C. Tian, J. Appl. Phys. **78**, 3965 (1995).

[25] H. Orihara and Y. Ishibashi, J. Phys. Soc. Jpn. **61**, 1919 (1992).

[26] H. Tomita and S. Miyashita, Phys. Rev. B **46**, 8886 (1992).

[27] P. A. Rikvold, H. Tomita, S. Miyashita, and S. W. Sides, Phys. Rev. E **49**, 5080 (1994).

[28] P. A. Rikvold and B. M. Gorman, in *Annual Reviews of Computational Physics I*, edited by D. Stauffer (World Scientific, Singapore, 1994), p. 149.

[29] H. M. Duiker and P. D. Beale, Phys. Rev. B **41**, 490 (1990).

[30] P. D. Beale, Integrat. Ferroelec. **4**, 107 (1994).

[31] H.-B. Braun, Phys. Rev. Lett. **71**, 3557 (1993); J. Appl. Phys. **75**, 4609 (1994); Phys. Rev. B **50**, 16 485 (1994); **50**, 16 501 (1994).

[32] C. Kittel, Phys. Rev. **70**, 965 (1946).

[33] R. Czech and J. Villain, J. Phys. Condens. Matter **1**, 619 (1989).

[34] B. Kaplan and G. A. Gehring, J. Magn. Magn. Mater. **128**, 111 (1993).

[35] A. B. MacIsaac, J. P. Whitehead, M. C. Robinson, and K. De'Bell, Phys. Rev. B **51**, 16 033 (1995).

[36] I. Booth, A. B. MacIsaac, J. P. Whitehead, and K. De'Bell, Phys. Rev. Lett. **75**, 950 (1995).

[37] K.-O. Ng and D. Vanderbilt, Phys. Rev. B **52**, 2177 (1995).

[38] R. Carey and E. D. Isaac, *Magnetic Domains and Techniques for their Observation* (Academic, New York, 1966).

[39] A. N. Kolmogorov, Bull. Acad. Sci. USSR Mat. Ser. **1**, 355 (1937).

[40] W. A. Johnson and P. A. Mehl, Trans. Am. Inst. Miner. Min. Eng. **135**, 365 (1939).

[41] M. Avrami, J. Chem. Phys. **7**, 1103 (1939); **8**, 212 (1940); **9**, 177 (1941).

[42] L. Onsager, Phys. Rev. **65**, 117 (1944).

[43] C. N. Yang, Phys. Rev. **85**, 809 (1952).

[44] S. Mørup, Hyperfine Interact. **90**, 171 (1994).
[45] U. Nowak, IEEE Trans. Magn. **31**, 4169 (1995).
[46] D. Townsley, M. A. Novotny, and P. A. Rikvold (unpublished).
[47] N. Metropolis *et al.*, J. Chem. Phys. **21**, 1087 (1953).
[48] R. J. Glauber, J. Math. Phys. **4**, 294 (1963).
[49] P. C. Hohenberg and B. Halperin, Rev. Mod. Phys. **49**, 435 (1977).
[50] P. A. Martin, J. Stat. Phys. **16**, 149 (1977).
[51] A. B. Bortz, M. H. Kalos, and J. L. Lebowitz, J. Comput. Phys. **17**, 10 (1975).
[52] M. A. Novotny, Comput. Phys. **9**, 46 (1995).
[53] E. Stoll and T. Schneider, Phys. Rev. A **6**, 429 (1972).
[54] L. S. Schulman, J. Phys. A **13**, 237 (1980).
[55] L. S. Schulman, in *Finite Size Scaling and Numerical Simulation of Statistical Systems*, edited by V. Privman (World Scientific, Singapore, 1990), p. 490.
[56] J. Lee, M. A. Novotny, and P. A. Rikvold, Phys. Rev. E **52**, 359 (1995).
[57] C. P. Bean and J. D. Livingston, J. Appl. Phys. **30**, 120S (1959).
[58] C. Domb, in *Phase Transitions and Critical Phenomena*, edited by C. Domb and J. L. Lebowitz (Academic, New York, 1974), Vol. 3.
[59] H. Furukawa and K. Binder, Phys. Rev. B **26**, 556 (1982).
[60] C. Rottman and M. W. Wortis, Phys. Rev. B **24**, 6274 (1981).
[61] R. K. P. Zia and J. E. Avron, Phys. Rev. B **25**, 2042 (1982).
[62] K. Leung and R. K. P. Zia, J. Phys. A **23**, 4593 (1990).
[63] K. Binder, Z. Phys. B **43**, 119 (1981).
[64] K. Binder, Phys. Rev. A **25**, 1699 (1982).
[65] B. Berg, U. Hansmann, and T. Neuhaus, Z. Phys. B **90**, 229 (1993).
[66] J. S. Langer, Ann. Phys. **41**, 108 (1967); Phys. Rev. Lett. **21**, 973 (1968); Ann. Phys. **54**, 258 (1969).
[67] N. J. Günther, D. A. Nicole, and D. J. Wallace, J. Phys. A **13**, 1755 (1980).
[68] C. C. A. Günther, P. A. Rikvold, and M. A. Novotny, Phys. Rev. Lett. **71**, 3898 (1993); Physica A **212**, 194 (1994).
[69] R. A. Ramos, S. W. Sides, P. A. Rikvold, and M. A. Novotny (unpublished).
[70] I. M. Lifshitz, Sov. Phys. JETP **15**, 939 (1962).
[71] S. K. Chan, J. Chem. Phys. **67**, 5755 (1977).
[72] S. M. Allen and J. W. Cahn, Acta Metall. **27**, 1085 (1979).
[73] J. A. N. Filipe, A. J. Bray, and S. Puri, Phys. Rev. E **52**, 6082 (1995).
[74] K. Sekimoto, Physica A **135**, 328 (1986).
[75] A. Milchev, K. Binder, and D. W. Heermann, Z. Phys. B **63**, 521 (1986).
[76] D. L. Mills, in *Ultrathin Magnetic Structures*, edited by J. A. C. Bland and B. Heinrich (Springer, New York, 1994), Vol. 1.
[77] H. L. Richards, M. Kolesik, P.-A. Lindgård, P. A. Rikvold, and M. A. Novotny (unpublished).
[78] M. Kolesik, M. A. Novotny, and P. A. Rikvold (unpublished).